Association Aéronautique et Astronautique de France

59th 3AF International Conference on Applied Aerodynamics
24 — 26 March 2025, Strasbourg – France

AERO2025-32-MRAZEK

Implementation and Validation of a Geometric Advection Scheme in a CLSVOF Solver

Tomas Mrazek[(1)], Yohei Sato[(2)], Chiara Manfletti[(1)]
[(1)]*Technical University of Munich, Arcisstraße 21, München 80333, Germany*
[(2)]*Paul Scherrer Institut, Forschungsstrasse 111, Villigen, 5232, Switzerland*
tomas.mrazek@tum.de, yohei.sato@psi.ch, chiara.manfletti@tum.de

ABSTRACT

In this work, a Coupled Level Set and Volume of Fluid (CLSVOF) solver using a geometric advection scheme is proposed and implemented. By improving droplet advection fidelity compared to existing methods, a reduction in the cost of characterising liquid breakup can be achieved, contributing to better fuel atomisation in propulsion systems. Validation of the solver is performed using a simple bubble advection case, where improved performance and field error compared to an algebraic CLSVOF implementation is noted. Verification is performed by replicating a planar airblast atomiser experiment. Here, good agreement with experimental results on breakup dynamics is observed along with clear improvement in droplet advection fidelity compared to algebraic methods. A comparison with a geometric VoF solver shows similar performance and accuracy due to the high Weber number flow. The `isoCLSVOFFoam` solver presented in this work presents a promising alternative to existing CLSVOF codes, particularly when good droplet resolution and surface tension modelling are required.

1. INTRODUCTION

Atomisation is a process by which a bulk liquid is disintegrated into small drops through exposure to high-velocity fluid or mechanical work. In real flows, breakup is highly three-dimensional and may occur in a multi-stage process of primary and secondary atomisation. The fluid-gas interface is subject to not only aerodynamic forces, but also variable viscosity and surface tension, all of which must be considered in an accurate simulation.

Predicting fluid breakup has applications in fields including agriculture, medicine, and meteorology. Crop spraying and additive manufacturing command specific drop sizes to control spray drift and layer thickness respectively [9, 19] . In medicine, atomisation is used for spray coating and surface treatments to improve drug delivery efficiency. In aerospace, atomisation is a key driver of efficient combustion. Modern gas turbines are operated at equivalence ratios that minimise smoke, unburned hydrocarbons (UHC), and NOx emissions. To this end, their fuel injectors maximise fuel surface area in order to increase evaporation, reaction rate and flame speed, allowing accurate control of the equivalence ratio [6]. In emerging lean combustion architectures, fuel injectors play a particularly important role in promoting stable combustion throughout the entire flight envelope [24].

Liquid breakup occurs when aerodynamic forces overcome surface tension at the critical Weber number - given in Eq. 1 to be a measure of the ratio of inertial to surface tension forces

$$\mathrm{We}_{crit} = \frac{8}{C_D} \tag{1}$$

Breakup in fuel injectors typically takes place in a primary and secondary stage. Primary atomisation describes bulk fluid breakup into ligaments or large droplets. For droplets and ligaments exceeding a critical size, secondary breakup occurs producing droplets that are aerodynamically stable, given by Eq. 2 .

$$D_{crit} = \frac{8\sigma}{C_D \rho U^2} \tag{2}$$

In modern prefilming airblast atomisers, fuel is introduced along a prefilmer and spread into a thin, expanding conical sheet. For such sheets, three disintegration modes have been identified - *rim*, *wave*, and *perforated sheet*. These modes have been observed to occur simul-

taneously as the liquid sheet grows thinner downstream and can no longer be maintained by surface tension [8].

Liquid breakup can be studied experimentally using employ optical or x-ray imaging techniques [5, 11]. However, these can be cost-prohibitive and constrained to non-reacting flows at lower Reynolds number and temperature. In contrast, simulations can promise faster and more affordable iteration with no prototyping cost.

Several approaches to modelling the liquid-gas interface in the Eulerian representation of fluid flow have been developed, the oldest of which is the Volume of Fluid (VoF) Method [10]. In this method α, representing the volume fraction of the fluid of interest, is advected along with the flow. However, advecting a fluid interface, represented by a step function, presents the challenge of balancing numerical diffusion and computational cost. The Level Set method [16], which is inherently continuous, allows for better calculation of surface normals and thus surface tension [21], but at the cost of numerical dissipation and thus a loss of mass conservation [13].

The recently introduced Coupled Level Set Volume of Fluid (CLSVOF) method [21] combines both approaches to achieve good mass and interface conservation. Most implementations of the CLSVOF method employ an algebraic advection scheme. Algebraic interface capturing schemes are comparatively simpler, but result in numerical diffusion and poor interface shape conservation. In this work, a CLSVOF solver employing a geometric advection scheme is implemented. The verification case involves the transport of a disc in a steady uniform flow, while the validation case focuses on a planar airblast atomiser.

2. NUMERICAL METHOD

2.1 Background

The fluid interface presents a discontinuity in the flow variables that varies with time. In Eulerian representations of fluid flow, this interface is imposed on a grid of cells that do not coincide exactly with the interface position. Accurate tracking and advection of the interface as it deforms is therefore required. To this end, several algorithms for interface tracking have been developed.

VoF methods, proposed by Hirt and Nichols (1979), treat fluid interfaces as discontinuous, giving oscillatory solutions of surface curvature and thus poor predictions of surface tension [10]. This is mitigated by smoothing, but at the cost of feature resolution. Level set methods, proposed by Osher and Sethian (1988) employ a continuous distance function that improves curvature prediction, but numerical dissipation results in loss of mass in regions enclosed by the zero level set [16]. To address the shortcomings of both methods, Coupled Level Set and Volume of Fluid (CLSVOF) methods first outlined by Sussman (2000) combine both approaches to achieve good interface tracking and mass conservation [21]. Implementations of a CLSVOF solver in OpenFOAM® have previously been presented by Menon (2016) and Yamamoto (2016) [14, 25].

Most implementations of the CLSVOF method use algebraic advection schemes such as `MULES` *(Multidimensional Universal Limiter for Explicit Solution)*. Algebraic interface advection is simpler to implement and less computationally demanding, but suffers from numerical diffusion, smearing the fluid interface cross several cells. Compared to geometric methods, `MULES` has been shown to distort the interface shape along mesh faces, as replicated in Section 3.1 of this work [18].

Geometric interface capturing algorithms are more complex, but result in a sharp fluid interface and better shape preservation of advected droplets. A geometric scheme has been implemented in the purely-VoF `interIsoFoam` solver in OpenFOAM® [18]. This scheme aims to minimise the number of operations performed by geometric advection schemes, which results in faster computation compared to algebraic schemes despite the more complex interface tracking implementation. Stability improvements of the `isoAdvector` scheme compared to `MULES` were noted by both the authors' and Pedersen (2017) [17]. It is therefore predicted that a CLSVOF solver implementing this scheme may outperform solvers employing algebraic advection, giving rise to the proposed implementation.

2.2 isoCLSVOFFoam Solver

This section describes the implementation of the Simple CLSVOF (S-CLSVOF) algorithm employed by `isoCLSVOFFoam`. It should be noted that other implementations of the CLSVOF method exist, and differ by the degree to which the LS and VoF methods are coupled. In the S-CLSVOF method proposed by Albadawi (2013), the VoF advection equation is solved and the LS field derived from it, which stands in contract to the standard CLSVOF implementation by Sussman (2000) where both equations are advected [21, 1].

In order to provide a complete overview of the algorithm, the principal governing equations of the VoF and LS methods are explained first, followed by an explanation of their coupling.

The VoF field represents a volume fraction $\alpha \in [0,1]$ of a fluid of interest, defined as a single scalar for each cell. A region of purely fluid A corresponds to $\alpha = 0$, purely fluid B to $\alpha = 1$, while intermediate values indicate a fluid interface. The expression for density is given in Eq. 3, showing that fluid properties at any given point are a function of α.

$$\rho = \alpha\rho_A + (1-\alpha)\rho_B \tag{3}$$

To advect α along with the flow without smearing the fluid interface, geometric or algebraic schemes may be used. Algebraic advection schemes such as `MULES` solve the advection Eq. 4 on the volume fraction α.

$$\frac{\partial \alpha}{\partial t} + \nabla \cdot (\alpha \mathbf{U}) = 0 \tag{4}$$

A limiter function to ensure monotonicity is implemented, as well as an interface compression step to improve interface sharpness. In `MULES`, Eq. 4 is modified to compress the interface and reduce smearing, then discretised and propagated for each cell. Due to the fluid interface being represented by discrete values of α, smoothing must be applied to avoid a stair-shaped approximation of the interface and thus an oscillatory solution for the interface normal vector [4].

In geometric advection schemes such as that implemented in this work, the fluid interface is represented by an isosurface. In the `isoAdvector` scheme, an isovalue f of the volume fraction $\alpha_i(t)$ is found for each surface cell i, for which the cell is divided into correct volume fractions of the two fluids. The movement of this isosurface during a timestep is estimated using the velocity field, which allows the calculation of the submerged face area at time $t + \Delta t$ and the total volume of fluid A transported across face i, ΔV_i. From this, the volume fraction $\alpha_i(t + \Delta t)$ is obtained. In case of $\alpha > 1$ or $\alpha < 0$, bounding is applied and α is redistributed among neighboring cells such that $0 < \alpha < 1$ for all cells, ensuring mass conservation. A detailed explanation of the `isoAdvector` algorithm is given in [18].

An alternative to the Volume of Fluid method, the Level Set method employs a signed distance function ϕ, called the level set function, to represent the two fluid phases [16]. Fluid A can be represented by $\phi > 0$, fluid B by $\phi < 0$, with the free surface represented by $\phi = 0$ (also known as the zero level set). The level set function is initialised as a signed distance from the fluid interface to any point in the computational domain. This function is then advected with time using Eq. 5.

$$\frac{\partial \phi}{\partial t} + \mathbf{U} \cdot \nabla \phi = 0 \tag{5}$$

Implementation by Sussman (1999) [20] represents surface tension as a body force using the Continuum approach developed by Brackbill et al. (1992) [2]. The surface curvature κ is given by Eq. 6.

$$\kappa = -\nabla \cdot \frac{\nabla \phi}{|\nabla \phi|} \tag{6}$$

The level set function is inherently continuous, improving prediction of interface normals and surface tension compared to VoF methods. Tracking of fluid separation is therefore possible without the need for explicit reconstruction. However, advection of ϕ gives rise to numerical dissipation. Gain or loss of mass is observed in regions enclosed by the zero level set, particularly in regions of high curvature or poor resolution [13]. This is a drawback compared to VoF's conservative finite difference methods. To alleviate numerical dissipation, higher order schemes are employed and the level set function is periodically reinitialised to ensure it continues to represent a signed distance function from the interface.

In `isoCLSVOFFoam`, the coupling between LS and VoF method addresses the deficiencies of both methods. The VoF field α is advected using the `isoAdvector` scheme as in `interIsoFoam`. The α field is then used to initialise the continuous level set field ϕ with $\phi_0 = 0$ at the interface, such that

$$\phi_0 = (2\alpha - 1)\Gamma \tag{7}$$

where Γ is a function of the mesh step size, $\Gamma = 0.75\Delta x$. This function is then re-distanced such that $|\nabla \phi| = 1$ using Eq. 8, where τ is an artificial timestep chosen as $\Delta\tau = 0.1\Delta x$.

$$\begin{cases} \frac{\partial \phi}{\partial \tau} = S(\phi_0)(1 - |\nabla \phi|), \\ \phi(\mathbf{x}, 0) = \phi_0(\mathbf{x}). \end{cases} \tag{8}$$

The surface normals are obtained from the gradient of ϕ and lead to Eq. 6 for the surface curvature κ. The surface tension can then be obtained using the aforementioned Continuum Surface Force (CSF) model by Brackbill [2], given by Eq. 9.

$$f_\sigma = \sigma \delta(\phi) \kappa(\phi) \nabla \phi \tag{9}$$

where δ is the Dirac function

$$\delta(\phi) = \begin{cases} \frac{1}{2\varepsilon}\left(1 + \cos\left(\frac{\pi\phi}{\varepsilon}\right)\right), & |\phi| \leq \varepsilon \\ 0, & |\phi| > \varepsilon \end{cases}$$

and σ the surface tension coefficient. In addition to correcting the surface tension, density and viscosity fields are corrected using the Heaviside function, which reduces the imbalance between surface tension and physical properties at the cost of worse mass conservation [25].

The *algebraic* S-CLSVOF solver `sclsVOFFoam` serves as a basis for this solver [25]. Modifications were made to `AlphaEqn.H` due to changes in the `MULES::correct()` syntax in recent versions of OpenFOAM®. The `isoCLSVOFFoam` solver is made publicly available [15].

2.3 Disc in Steady Uniform Flow

The first of two validation cases features a disc of one phase ($\alpha = 0$) advected through a domain of another phase ($\alpha = 1$). Tab. 1 details the simulation setup. An initial flow of $\mathbf{U} = (1, 0.5)$ is prescribed, with the same velocity vector imposed along the structure domain's extremities using a `fixedValue` boundary condition. The disc travels from the lower left corner to the upper right

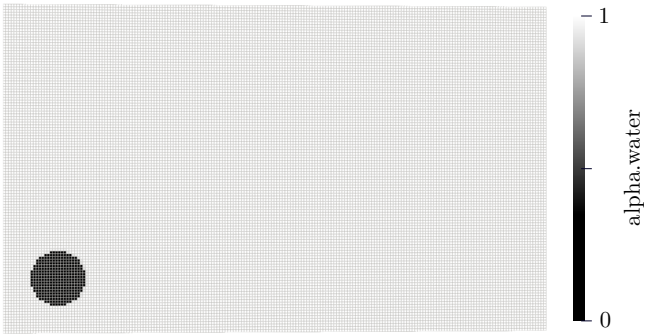

Figure 1: Domain with initial disc shape.

corner of the two-dimensional domain, shown in Fig. 4.1. Simulation time is 4 seconds, and the $\text{CFL}_{max} = 0.5$. The shape and volume, as well as interface and runtime are compared for each solver.

Domain size (mm)	50×30
Domain resolution	200×120
Disc Radius R (mm)	2.5
Disc initial position (mm)	$(5, 5)$
Disc final position (mm)	$(45, 25)$

Table 1: Simulation setup

The setup follows a reference study by Roenby (2016) [18]. In this study, the `isoAdvector` geometric scheme was proposed and compared against `MULES`, `HRIC`, and `CICSAM`, the latter two featured in commercial codes StarCCM+® and Ansys FLUENT® respectively. The `MULES` advection scheme is employed in `interFoam` as well as the coupled `sclsVOFFoam` solver by Yamamoto [25]. The latter solver uses `MULES` to advect the α field, calculating the LS function ϕ from the result of this advection. The `isoCLSVOFFoam` solver investigated in this work employs the `isoAdvector` scheme instead.

In the reference study, the `isoAdvector` scheme showed improvement in shape preservation, achieving a minimum factor of 7 reduction in average error. Moreover, computation time was reduced by a factor of between 2 and 4. Qualitatively, `MULES` exhibited a tendency to distort the advected interface at 45° to the mesh faces. This was somewhat mitigated when an unstructured mesh was used, as cell normal directions were no longer consistent and this tendency was averaged out.

In the *"Disc in steady uniform flow"* case, not only the advection equation for the phase index, but also the momentum equations were solved. In the reference study by Roenby (2016), only the phase advection equations were solved by applying the `frozenFlow` parameter in OpenFOAM®'s `PIMPLE` sub-dictionary. The aim of this change was to understand the impact of different advection schemes on *overall* simulation time for a simple 2D atomisation simulation. Three solvers are compared in this study - `interIsoFoam`, `sclsVOFFoam`, and `isoCLSVOFFoam`. Thus, a comparison is obtained between a pure VoF solver, a coupled LS and VOF solver with algebraic advection, and a coupled LS and VOF solver with geometric advection.

2.4 Planar Airblast Atomiser

In this test case, the breakup of a liquid sheet emulating a fuel injector section is studied. The case mirrors a liquid sheet generator at ONERA, where a NACA63-010 aerofoil with $c = 89$ mm and a 300 µm tall slit at its trailing edge is used to introduce a liquid into a stream of air [12, 7]. A wedge system allows for the flow area at the injection point to be modified, allowing for control of the pressure gradient and Reynolds number at this point.

The particular experiment replicated in this work was performed by Déjean et al. (2006) [3] with the purpose of studying the impact of fluid and air thickness on primary atomisation. Water was introduced into a domain with a restricted 9 mm passage at the injection point, forming converging flow profile (case C9 in [3], shown in Fig. 2).

Case C9 is particularly suitable for validation of a multiphase solver, as the converging flow profile was experimentally demonstrated to maintain laminar flow over the wing's surface by creating a favorable pressure gradient. Consequently, a coarser mesh upstream of the injector where no atomisation takes place can be used. The absence of a prefilmer decouples liquid breakup from turbulent film development, which was found by Wetherell (2024) to double the modal ligament length and increase the Sauter Mean Diameter (SMD), requiring a separate costly simulation to model [23].

Existing work by Villedieu (2013) replicating this experimental configuration using the two-fluid SLOSH code provides an additional point of comparison [22]. In this computational study, good agreement with experiment was observed with respect to breakup length, but flapping frequency was overestimated, as was the amplitude of velocity fluctuations downstream of the aerofoil. The authors suggested that some of the 3D flow structures present in the experiment were not well represented by the 2D simulation.

The domain, recreated from [3] and [22], spans 0.69 m by 0.6 m, much of which is the downstream region. The trailing edge of the aerofoil was trimmed to a thickness of 2 mm. Fig. 3 shows the overall domain, while Fig. 2 gives the dimensions near the inlet and injector. All downstream boundaries were treated as pressure outlets.

Due to computational constraints, the domain is a two-dimensional representation of configuration C9. Five cells span the liquid sheet thickness, giving $\Delta x = 60$ µm at the injection point as well as within a 40 mm refinement

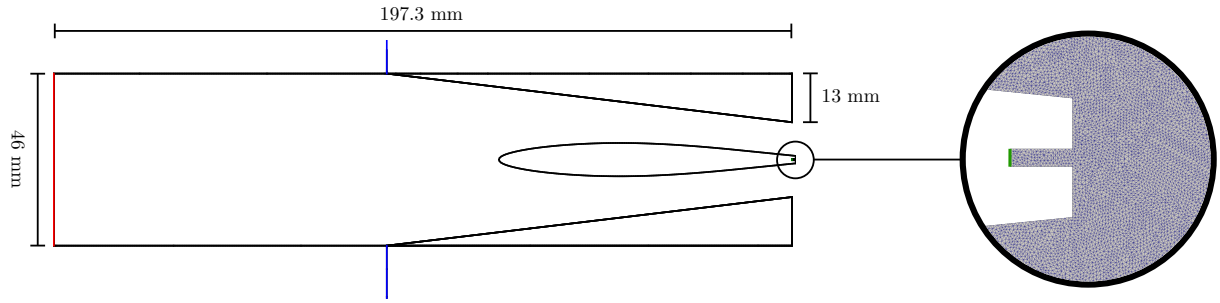

Figure 2: Domain near-field region and mesh near trailing edge. Air inlet denoted in red, pressure outlets in blue, water inlet in green, and no-slip walls in black.

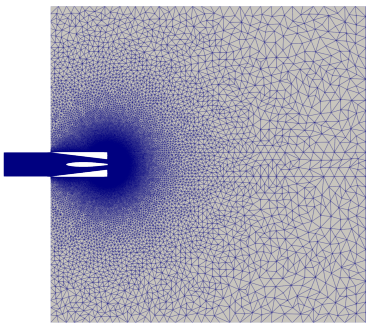

Figure 3: 2D mesh of the complete domain.

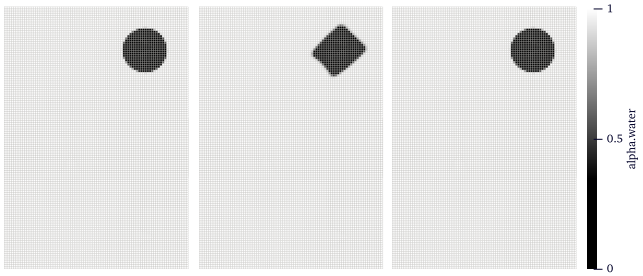

Figure 4: Final position and shape of disc after 4 seconds. Left to right: `interIsoFoam`, `sclsVOFFoam`, and `isoCLSVOFFoam`.

radius, in order to fully resolve the breakup process. The resulting mesh contains 3.9 million cells.

A constant air inlet mass flux rate of 13.97 $\mathrm{kg\,s^{-1}\,m^{-2}}$ was prescribed, corresponding to a velocity of 50 $\mathrm{m\,s^{-1}}$ at the injection point. Water was introduced with a Poiseuille profile with an average velocity of 2.2 $\mathrm{m\,s^{-1}}$, realized using a `groovyBC` expression provided by the `swak4foam` library. The boundary conditions selected match those used by Villedieu (2013) [22]. The timestep was determined by the CFL criterion, which was limited to 0.5 across the fluid boundary using the `maxAlphaCo` parameter.

3. RESULTS AND DISCUSSION

In this section, the proposed `isoCLSVOFFoam` solver, which is a CLSVOF method incorporating a geometric VoF scheme, is compared against a geometric VoF solver (`interIsoFoam`) and a CLSVOF solver utilizing an algebraic VoF (`sclsVOFFoam`).

3.1 Disc in Steady Uniform Flow

The final position and shape of the advected disc for each of the three solvers is shown in Fig. 4. In the `sclsVOFFoam` case, the disc was distorted at 45° angles to the mesh cell faces, with a shape resembling a diamond. This is consistent with findings by Roenby (2016) [18]. The results in this figure can be directly compared to Figure 4 of the reference study, with a maximum Courant number of 0.2 applied in both cases. This result, along with the good shape preservation achieved by the derived `isoCLSVOFFoam` solver suggests the `MULES` advection scheme is responsible for this distortion.

To quantify the difference in advection accuracy, a mean field error was calculated. As the velocity throughout the domain, including boundary conditions, was prescribed to $\mathbf{U} = (1, 0.5)$, the disc should be uniformly displaced to $(4.5, 2.5)$. Compared to this expected flowfield, created by displacing the initial disc to its final position, a field-averaged error was calculated using Equation 10,

$$E = \frac{\sum_i |\alpha_i - \alpha_{i,exp}|}{\sum_i \alpha_{i,exp}} \tag{10}$$

where the *exp* subscript refers to the expected flowfield. Volume averaging was not required due to the uniform mesh used. The field-averaged error is given in Table 2. The identical error E for `interIsoFoam` and `isoCLSVOFFoam` is attributed to the limited benefit of the LS method for this case. Tab. 2 shows an order of magnitude difference in error between the `MULES` and `isoAdvector` schemes, in line with differences observed by Roenby (2016) for a frozen flow case [18].

The runtime of each solver was recorded to assess the

	interIso	sclsVOF	isoCLSVOF
E	3.89×10^{-4}	2.50×10^{-3}	3.89×10^{-4}
t (s)	230.44	270.12	233.04

Table 2: Error E and CPU time t for each solver

impact the coupled LS method, as well as the change in advection scheme has on the overall solution time of a simple case with interface advection as well as pressure and velocity calculation. `interIsoFoam` achieves the lowest runtime, not calculating the LS field ϕ. The coupled level set method under the same advection scheme, represented by `isoCLSVOFFoam` is only 1% slower. Comparing `sclsVOFFoam` against `isoCLSVOFFoam` indicates that the replacement of `isoAdvector` with `MULES` increased runtime by 16%.

3.2 Planar Airblast Atomiser

The Planar Airblast Atomiser case was evaluated for $t = 12$ms. Data was averaged over a time window of $t = [0.00425, 0.01185]$ s to allow flow propagation downstream of the injector and the development of a periodic breakup pattern. Tab. 4 compares the runtime and average timestep for all three solvers, as extracted from OpenFOAM®'s structured log. The additional computation of the LS field increases $\bar{\Delta t}$ by 19 and 20% for `sclsVOFFoam` and `isoCLSVOFFoam` respectively.

In Section 3.1, the proposed achieved significantly lower CPU time than `sclsVOFFoam`, a result not replicated here. The `isoAdvector` scheme's performance advantage is more prominent with structured meshes, such as that used in Section 3.1 [18]. On unstructured meshes like that used in this case, the advantage shrinks due to the more complex process of isosurface computation.

	interIso	sclsVOFF	isoCLSVOF
$\bar{A}$ (mm^2)	0.86	0.15	0.88
$N_{droplets}$	33.2	7.1	31.2

Table 3: Droplet size and number at $x = [24, 26]$ mm

The flapping frequency in Tab. 5 was obtained by extracting the maximum y-coordinate of the liquid sheet at $x = 5.0$ mm (marked on Fig. 7) at a frequency of 10 kHz and fitting a least squares sine fit rather than a Fourier transform due to the small window of data available. Due to computational constraints, a longer simulation time was not possible. Comparing the flapping frequency to the reference experimental study by Déjean (2013) [3], agreement is observed within the uncertainty in f for `interIsoFoam` and `isoCLSVOFFoam`. Better agreement with experiment is observed compared to the SLOSH

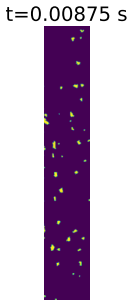

Figure 5: Droplet recognition mask downstream of the domain for `isoCLSVOFFoam`

code investigated by Villedieu (2013) [22], but a large uncertainty in f prevents definitive conclusions. Weakly periodic behaviour was observed with `sclsVOFFoam`, the sine function giving a poor fit and the Fourier transform giving no distinct frequency peaks.

Breakup length L_b represents the mean continuous length of the liquid sheet. Comparing `interIsoFoam` and `isoCLSVOFFoam` in Tab. 5, longer breakup length and better agreement with experiment is observed in the purely-VoF solver. The higher flapping frequency and shorter breakup length observed with `isoCLSVOFFoam` are linked, with more frequent breakup events preventing longer ligament formation. All computational results appear to underestimate the breakup length, which may point to the 3D fluid breakup not being fully represented by the 2D simulations performed.

Accurately modelling secondary atomisation is essential to establishing boundary conditions for combustion simulations downstream of the injector. For a slice of the domain $x = [24, 26]$ mm, statistics of number of droplets and their area were performed to assess the fidelity of droplet advection. A mask corresponding to $\alpha = 0$ was subtracted from the domain data, shown in 5. Distinct regions were labelled and their area measured using the `scikit.measure` library. Similar droplet number and size distributions were observed for solvers using the `isoAdvector` scheme. The similar performance of the `interIsoFoam` and `isoCLSVOFFoam` solvers throughout this case may be a result of the relatively weak coupling between the VoF and LS methods explained in Section 2.2. Furthermore, the *Planar Airblast Atomiser* case is inertia dominated rather than surface tension dominated, and thus does not benefit as much from improved prediction of surface tension. The apparent difference would likely increase with a decrease in the case Weber number. On the other hand, `sclsVOFFoam` did not advect discrete droplets, instead diffusing the atomised water into regions of higher and lower concentration, as seen in Fig. 6.

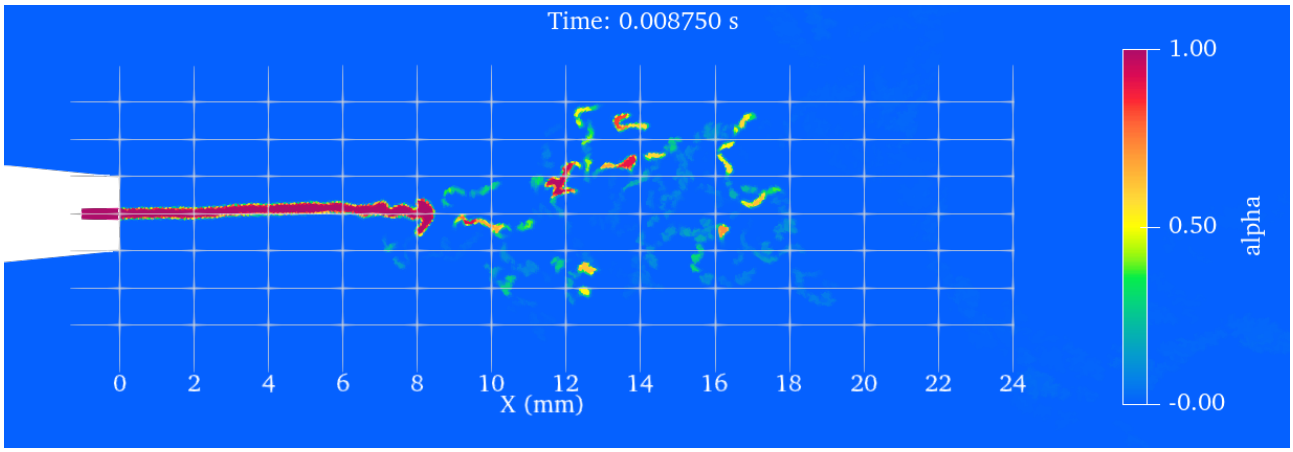

Figure 6: Flowfield at $t = 8.75$ ms obtained by the `sclsVOFFoam` solver.

	interIso	sclsVOFF	isoCLSVOF
Average Timestep $\bar{\Delta t}$ (s)	2.26×10^{-7}	2.46×10^{-7}	2.12×10^{-7}
Average Time $\bar{t}$ per iteration (s)	10.48	12.45	12.61

Table 4: Runtime statistics extracted from OpenFOAM®'s structured log.

	interIso	sclsVOFF	isoCLSVOF	Déjean (2013) [3]	Villedieu (2013) [22]
Flapping Frequency f (Hz)	335	189	376	355	510
Breakup length $\bar{L_b}$ (mm)	10.8	8.9	9.6	13.5	10.5

Table 5: Droplet breakup dynamics comparison to reference computational and experimental results.

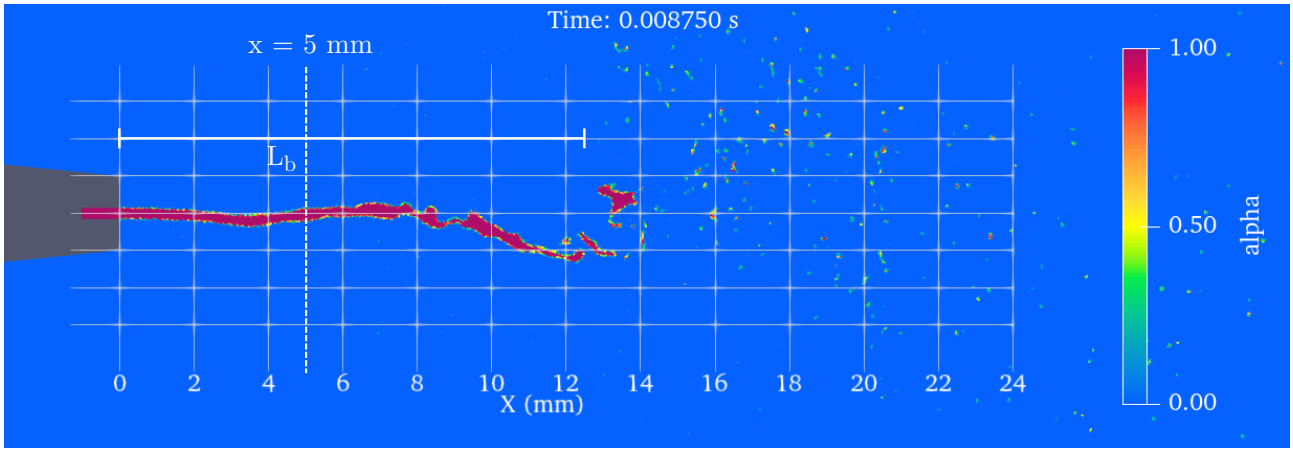

Figure 7: Flowfield at $t = 8.75$ ms obtained by the `isoCLSVOFFoam` solver.

4. CONCLUSION

The objective of this study was to implement a geometric advection scheme in a S-CLSVOF solver and evaluate its performance in simulating liquid atomisation. Building on an existing algebraic S-CLSVOF code, the `isoCLSVOFFoam` solver was implemented and compared to an a geometric VoF (`interIsoFoam`) and algebraic S-CLSVOF (`sclsVOFFoam`) solver.

Validation was performed using a simple bubble advection case, where comparable CPU time and accuracy to a geometric VoF solver was observed, reducing simulation time by 14% compared to the existing `sclVOFFoam` code.

Verification was performed by replicating a planar airblast atomiser experiment at ONERA. The liquid breakup process was described using the flapping frequency, breakup length, droplet shape, and number downstream of the injector. In this regard, good agreement with experimental data was observed, as well as significant improvement over algebraic S-CLSVOF, particularly in droplet resolution. Challenges with simulation time needed to extract meaningful spray statistics were highlighted. The geometric `interIsoFoam` code showed similar performance to the proposed solver, suggesting that for cases where inertial forces dominate surface tension a VoF approach may be sufficient.

With this in mind, the solver implemented in this work offers clear improvement over existing algebraic S-CLSVOF for the validation and verification cases, showing good agreement with experiment. For cases with significant surface tension forces that require good droplet resolution, `isoCLSVOFFoam` presents a promising option with computational performance comparable to VoF methods.

REFERENCES

[1] A. Albadawi, D.B. Donoghue, A.J. Robinson, D.B. Murray, and Y.M.C. Delauré. Influence of surface tension implementation in volume of fluid and coupled volume of fluid with level set methods for bubble growth and detachment. *International Journal of Multiphase Flow*, 53:11–28, July 2013.

[2] J.U Brackbill, D.B Kothe, and C Zemach. A continuum method for modeling surface tension. *Journal of Computational Physics*, 100(2):335–354, June 1992.

[3] B. Déjean, P. Berthoumieu, and P. Gajan. Experimental study on the influence of the liquid and air thicknesses on a planar air-blasted liquid sheet. In *25th European Conference - Liquid Atomization & Spray Systems - ILASS 2013*, CHANIA, Greece, September 2013.

[4] Suraj S Deshpande, Lakshman Anumolu, and Mario F Trujillo. Evaluating the performance of the two-phase flow solver interfoam. *Computational Science amp; Discovery*, 5(1):014016, November 2012.

[5] Christophe Dumouchel. On the experimental investigation on primary atomization of liquid streams. *Exp. Fluids*, 45(3):371–422, September 2008.

[6] G.M. Faeth. Current status of droplet and liquid combustion. *Progress in Energy and Combustion Science*, 3(4):191–224, January 1977.

[7] V. Fernandez, P. Berthoumieu, and G. Lavergne. Preliminary atomization in water and kerozene liquid sheets at high pressure. In *11th ICLASS Conference*, Vail, Colorado, July 2009.

[8] R P Fraser, N Dombrowski, and J H Routley. The atomization of a liquid sheet by an impinging air stream. *Chem. Eng. Sci.*, 18(6):339–353, June 1963.

[9] Emilia Hilz and Arnoldus W.P. Vermeer. Spray drift review: The extent to which a formulation can contribute to spray drift reduction. *Crop Protection*, 44:75–83, February 2013.

[10] C. W. Hirt and Nichols B. D. Volume of fluid (vof) method for the dynamics of free boundaries. *Journal of Computational Physics*, 39:201–225, 1981.

[11] A L Kastengren, C F Powell, T Riedel, S-K Cheong, K-S Im, X Liu, Y J Wang, and J Wang. Nozzle geometry and injection duration effects on diesel sprays measured by x-ray radiography. *J. Fluids Eng.*, 130(4):041301, April 2008.

[12] C. Larrcq, P. Berthoumieu, G. Lavergne, and F. Thivet. Improvement of Airblast injectors with electroaerdynamic actuators. In *2nd International Symposium on Non Equilibrium Processes, Combustion and Atmospheric Phenomenon*, 2005.

[13] Frank Losasso, Ronald Fedkiw, and Stanley Osher. Spatially adaptive techniques for level set methods and incompressible flow. *Computers amp; Fluids*, 35(10):995–1010, December 2006.

[14] Sankar Menon. Couled level-set with vof interfoam. Doctoral thesis, Chalmers University of Technology, jan 2016.

[15] T. Mrazek. sclsvoffoam. https://github.com/tommrazek/sclsVOFFoam, 2024.

[16] S. Osher and J. A. Sethian. Fronts propagating with curvature-dependent speed: algorithms based on hamilton-jacobi formulations. *Journal of Computational Physics*, 79:12–49, 1988.

[17] Johan Rønby Pedersen, Bjarke Eltard Larsen, Henrik Bredmose, and Hrvoje Jasak. A new volume-of-fluid method in openfoam. 2017.

[18] Johan Roenby, Henrik Bredmose, and Hrvoje Jasak. A computational method for sharp interface advection. *Royal Society Open Science*, 3(11):160405, November 2016.

[19] Shaik Himam Saheb, Vinay Kumar Durgam, and A. Chandrashekhar. A review on metal powders in additive manufacturing. In *AIP Conference Proceedings*. AIP Publishing, 2020.

[20] Mark Sussman, Ann S Almgren, John B Bell, Phillip Colella, Louis H Howell, and Michael L Welcome. An adaptive level set approach for incompressible two-phase flows. *Journal of Computational Physics*, 148(1):81–124, January 1999.

[21] Mark Sussman and Elbridge Gerry Puckett. A coupled level set and volume-of-fluid method for computing 3d and axisymmetric incompressible two-phase flows. *Journal of Computational Physics*, 162(2):301–337, August 2000.

[22] P. Villedieu, G. Blanchard, and D. Zuzio. Numerical simulation of primary atomization of a sheared liquid sheet. Part 2: Comparison with experimental results. In *25th European Conference Liquid Atomization & Spray Systems - ILASS 2013*, CHANIA, Greece, September 2013.

[23] Jack R. J. Wetherell and Andrew Garmory. The effect of film development on primary breakup in a prefilming airblast atomizer. *Journal of Engineering for Gas Turbines and Power*, 146(9), March 2024.

[24] Günter Wilfert, Joerg Sieber, Andrew Rolt, Nick Baker, Armel Touyeras, and Salvatore Colantuoni. New environmental friendly aero engine core concepts. *ISABE Paper*, (2007-1120), 2007.

[25] Takuya Yamamoto, Yasunori Okano, and Sadik Dost. Validation of the s-clsvof method with the density-scaled balanced continuum surface force model in multiphase systems coupled with thermocapillary flows. *International Journal for Numerical Methods in Fluids*, 83(3):223–244, June 2016.